ACTA TECHNICA ČSAV

2 ročník 19 | 1974

ACADEMIA • PRAHA

ACTA TECHNICA ČSAV

ROČNÍK 19 - 1974

Vydává:

Československá akademie věd v Praze

Vedoucí redaktor:

Akademik BEDŘICH HELLER

Výkonný redaktor:

MARTA KAČEROVSKÁ

Redakce:

162 00 Praha 6 - Dolní Liboc, Braškovská 13

Administrace a expedice:

Poštovní novinový úřad, Jindřišská 14, 125 05 Praha 1

ANALYSIS OF STRUCTURALLY ORTHOTROPIC BRIDGE DECK SYSTEMS WITH STIFFENED OUTER EDGES

RICHARD BAREŠ

1. INTRODUCTION

The concept of idealizing the true, structurally orthotropic plane system by an equivalent orthotropic plate, having continuously distributed elastic rigidities per unit of distance in the two directions X and Y, is applicable also in the case when the edges have different stiffness than the inner portion of the over-all cross section of the bridge desk. Such systems are quite frequent in bridge construction, the longitudinal edges being often stiffened by special edge beams, or the outer beams having a different section than the interior beams, etc. The analysis is greatly facilitated when we apply the method of dimensionless coefficients [1], by means of which all the internal forces are easy to compute for any case of external – usually vertical – loading. In analysing the effects of edge-stiffening, we have first to express the transverse rotations at the free longitudinal edges as produced due to the external load, as well as such effects as induced in the system by transverse moment loading applied at the free edges.

2. EDGE ROTATIONS DUE TO EXTERNAL LOADS

The transverse rotation at the edge, as produced there by external loading is defined by the first partial derivative of the vertical deflection w with respect to y. Using the relations given in [1], we find – after some rearranging – that for the special case of a harmonic line load $p(x) = \sum_m p_m \sin m\pi x/l$ the rotations at the edges $\pm b$ of the structurally orthotropic plane structure are given by the expression (see fig. 1)

$$\beta(\pm b) = \sum_m \frac{p_m l^2}{4\sqrt{(\varrho_T \varrho_P)}\,\pi^2 m^2} \left[\tau(y)_m\right]_{y=\pm b} \sin \frac{m\pi x}{l}. \tag{1}$$

The dimensionless parameter τ in Eq. (1) has been discussed in [1], where also its numerical values are given, as depending on the following three dimensionless parameters: on the parameter of lateral stiffness $\vartheta = b/l\sqrt[4]{(\varrho_T/\varrho_P)}$ on the parameter of torsional stiffness $\alpha = (\gamma_T + \gamma_P)/[2(1+\eta)\sqrt{\varrho_T\varrho_P}]$ or upon the coefficient of the middle member in the Huber Equation $\varepsilon = [\eta + \alpha(1-\eta)]$ and on the parameter of contraction ability $\eta = \nu_T\sqrt{(\varrho_P/\varrho_T)}$. The location ordinates of anyone point under consideration are represented also by dimensionless parameters of location $\varphi = \pi y/b$ and $\psi = \pi e/b$. In all the above formulae the symbols ϱ_T, ϱ_P, γ_T, and γ_P denote the flexural and torsional rigidities for the directions X and Y, while ν_T denotes the transverse contraction coefficient of the material for the given structure.

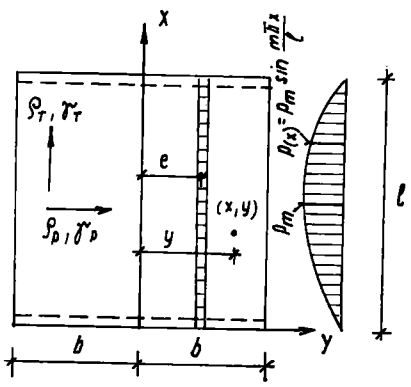

Fig. 1.

When a harmonic load evenly distributed over the width of the structure is considered, we find, similarly, for the transverse rotations at the edges the expression

$$\beta^0(\pm b) = \sum_m \frac{p_m^0 l^2 b}{\sqrt{(\varrho_T\varrho_P)}\,\pi^3 m^3}\,\eta[\tau^0(y)_m]_{\pm b}\sin\frac{m\pi x}{l}, \tag{2}$$

where the dimensionless factor τ^0, depending on ϑ, α, η, and φ is again to be found in [1], where also its numerical values are given.

3. EFFECTS OF TRANSVERSE EDGE MOMENTS

With regard to the torsional stiffness of the edge beams or of the outer beams, we have now to investigate the effects as produced across the system by edge moments acting in transverse direction; the effects to be considered are the deflection w, the edge rotations β and the transverse bending moments M_P.
When along the edges we apply external transverse moments, harmonic along X, i.e.

$$M = \sum M_m \sin\frac{m\pi x}{l} \tag{3}$$

then, in the absence of all external load between the two edges, the deflection at

anyone point is given directly by the homogeneous part of the solution to the Huber equation; thus

$$(4)\qquad w(x,y)_m = \{e^{mny}[\mathfrak{A}_m \cos mty + \overline{\mathfrak{B}}_m \sin mty] + e^{-mny}[\mathfrak{C}_m \cos mty + \overline{\mathfrak{D}}_m \sin mty]\} \sin \frac{m\pi x}{l}$$

where

$$t = \omega\sqrt{\left(\frac{1-\varepsilon}{2}\right)},\quad n = \omega\sqrt{\left(\frac{1+\varepsilon}{2}\right)},\quad \omega = \frac{\pi\vartheta}{b},$$

$$\overline{\mathfrak{B}} = \frac{\mathfrak{B}_m}{\sqrt{\left(\frac{1-\varepsilon}{2}\right)}},\quad \overline{\mathfrak{D}} = \frac{\mathfrak{D}_m}{\sqrt{\left(\frac{1-\varepsilon}{2}\right)}}.$$

For the case that the external edge moments are symmetrical (antisymmetrical), the deflection curve in the transverse direction is also symmetrical (antisymmetrical), and Eq. (4) reduces in this case to the form

$$(5)\qquad w^S(x,y)_m = \{\mathfrak{A}_m^S \operatorname{ch} mny \cos mty + \overline{\mathfrak{B}}_m^S \operatorname{sh} mny \sin mty\} \sin \frac{m\pi x}{l},$$

or to the form

$$(6)\qquad w^A(x,y)_m = \{\mathfrak{C}_m^A \operatorname{sh} mny \cos mty + \overline{\mathfrak{D}}_m^A \operatorname{ch} mny \sin mty\} \sin \frac{m\pi x}{l}.$$

Of the latter two equations Eq. (5) pertains to the symmetrical case, while Eq. (6) describes the antisymmetrical case.

The integration constants $\mathfrak{A}_m^S$, $\mathfrak{B}_m^S$, $\mathfrak{C}_m^A$, and $\mathfrak{D}_m^A$ have to be found from the conditions at the two boundaries $y = \pm b$ where we have

$$(7)\qquad 1.\ M_{Pm} = M_m \sin \frac{m\pi x}{l} \qquad \text{for } y = \pm b, \text{ i.e.}$$

$$\left[-\varrho_P \frac{\partial^2 w}{\partial y^2} - \eta\sqrt{(\varrho_T \varrho_P)}\,\frac{\partial^2 w}{\partial x^2} = M_m \sin \frac{m\pi x}{l}\right]_{y=\pm b}$$

$$(8)\qquad 2.\ \overline{Q}_{Pm} = \frac{\partial M_{Pm}}{\partial y} - \frac{\partial M_{TPm}}{\partial x} + \frac{\partial M_{PTm}}{\partial y} = 0 \quad \text{for } y = \pm b, \text{ i.e.}$$

$$\left[\frac{\partial^3 w}{\partial y^3} + \sqrt{\frac{\varrho_T}{\varrho_P}}(2\varepsilon - \eta)\,\frac{\partial^3 \omega}{\partial x^2\,\partial y} = 0\right]_{y=\pm b}.$$

Thus we have first to compute the respective derivatives of Eq. (5) and (6) as indicated in Eq. (7), and (8). Introducing the new symbols

$$n' = \vartheta \sqrt{\left(\frac{1+\varepsilon}{2}\right)}, \quad t' = \vartheta \sqrt{\left(\frac{1-\varepsilon}{2}\right)}, \quad \sigma = \pi\vartheta$$

we substitute the derivatives into the boundary conditions (7) and (8); rearranging, we obtain the equations needed for computing the integration constants. Considering the first of the boundary conditions as interpreted by Eq. (7), we write this equation for the edge $y = b$ and obtain

$$(9) \quad -\frac{M_m}{m^2 \varrho_P \omega^2} = \mathfrak{A}_m^S[(\varepsilon - \eta) \operatorname{ch} mnb \cos mtb - \sqrt{(1-\varepsilon^2)} \operatorname{sh} mnb \sin mtb] + \\ + \overline{\mathfrak{B}}_m^S[(\varepsilon - \eta) \operatorname{sh} mnb \sin mtb + \sqrt{(1-\varepsilon^2)} \operatorname{ch} mnb \cos mtb] .$$

From the second boundary condition as given by (8), we find for the edge $y = b$, similarly

(10)

$$-\mathfrak{A}_m^S\left[(1-\eta)\sqrt{\left(\frac{1+\varepsilon}{2}\right)} \operatorname{sh} mnb \cos mtb + (1+\eta)\sqrt{\left(\frac{1-\varepsilon}{2}\right)} \operatorname{ch} mnb \sin mtb\right] +$$

$$+\overline{\mathfrak{B}}_m^S\left[(1+\eta)\sqrt{\left(\frac{1+\varepsilon}{2}\right)} \operatorname{sh} mnb \cos mtb - (1-\eta)\sqrt{\left(\frac{1+\varepsilon}{2}\right)} \operatorname{ch} mnb \sin mtb\right] = 0 .$$

Solving these two equations for the unknown integration constants $\mathfrak{A}_m^S$, $\overline{\mathfrak{B}}_m^S$ we obtain

$$(11) \quad \mathfrak{A}_m^S = -\frac{M_m b^2}{m^2 \varrho_P \sigma^2} \frac{\mathfrak{G}_m^S}{\mathfrak{E}_m + \mathfrak{F}_m} .$$

$$(12) \quad \overline{\mathfrak{B}}_m^S = -\frac{M_m b^2}{m^2 \varrho_P \sigma^2} \frac{\mathfrak{H}_m^S}{\mathfrak{E}_m + \mathfrak{F}_m} ,$$

where

$$(13) \quad \mathfrak{G}_m^S = (1+\eta) \operatorname{sh} mn'\pi \cos mt'\pi - (1-\eta)\sqrt{\left(\frac{1+\varepsilon}{1-\varepsilon}\right)} \operatorname{ch} mn'\pi \sin mt'\pi ,$$

$$\mathfrak{H}_m^S = (1-\eta)\sqrt{\left(\frac{1+\varepsilon}{1-\varepsilon}\right)} \operatorname{sh} mn'\pi \cos mt'\pi + (1+\eta) \operatorname{ch} mn'\pi \sin mt'\pi ,$$

$$\mathfrak{E}_m = [(1+2\varepsilon) - \eta(2+\eta)] \operatorname{sh} mn'\pi \operatorname{ch} mn'\pi$$

$$\mathfrak{F}_m = [(1-2\varepsilon) + \eta(2-\eta)]\sqrt{\left(\frac{1+\varepsilon}{1-\varepsilon}\right)} \sin mt'\pi \cos mt'\pi .$$

Considering now the antisymmetrical case we use Eq. (7); writing it for the edge $y = b$ we obtain

$$(14)\quad -\frac{M_m}{m^2\varrho_P\omega^2} = \mathfrak{C}_m^A[(\varepsilon-\eta)\,\mathrm{sh}\,mnb\cos mtb - \sqrt{(1-\varepsilon^2)}\,\mathrm{ch}\,mnb\sin mtb] + \\ + \overline{\mathfrak{D}}_m^A[\sqrt{(1-\varepsilon^2)}\,\mathrm{sh}\,mnb\cos mtb + (\varepsilon-\eta)\,\mathrm{ch}\,mnb\sin mtb]\,.$$

Similarly, using Eq. (8) and writing this equation for the edge $y = b$, we find

$$-\mathfrak{C}_m^A\left[(1-\eta)\sqrt{\left(\frac{1+\varepsilon}{2}\right)}\,\mathrm{ch}\,mnb\cos mtb + (1+\eta)\sqrt{\left(\frac{1-\varepsilon}{2}\right)}\,\mathrm{sh}\,mnb\sin mtb\right] + \\ + \overline{\mathfrak{D}}_m^A\left[(1+\eta)\sqrt{\left(\frac{1-\varepsilon}{2}\right)}\,\mathrm{ch}\,mnb\cos mtb - (1-\eta)\sqrt{\left(\frac{1+\varepsilon}{2}\right)}\,\mathrm{sh}\,mnb\sin mtb\right] = 0\,.$$

On solving the latter two equations (14) and (15) simultaneously we obtain for the integration constants the expressions

$$(16)\quad \mathfrak{C}_m^A = -\frac{M_m b^2}{m^2\varrho_P\sigma^2}\,\frac{\mathfrak{G}_m^A}{\mathfrak{E}_m - \mathfrak{L}_m}\,,$$

$$(17)\quad \overline{\mathfrak{D}}_m^A = -\frac{M_m b^2}{m^2\varrho_P\sigma^2}\,\frac{\mathfrak{H}_m^A}{\mathfrak{E}_m - \mathfrak{F}_m}\,,$$

Here the factors $\mathfrak{E}$ and $\mathfrak{F}$ are defined as in (13), and

$$(18)\quad \mathfrak{G}_m^A = (1+\eta)\,\mathrm{ch}\,mn'\pi\cos mt'\pi - (1-\eta)\sqrt{\left(\frac{1+\varepsilon}{1-\varepsilon}\right)}\,\mathrm{sh}\,mn'\pi\sin mt'\pi$$

$$\mathfrak{H}_m^A = (1-\eta)\sqrt{\left(\frac{1+\varepsilon}{1-\varepsilon}\right)}\,\mathrm{ch}\,mn'\pi\cos mt'\pi + (1+\eta)\,\mathrm{sh}\,mn'\pi\sin mt'\pi\,.$$

Having thus found the constants $\mathfrak{A}^S$, $\mathfrak{B}^S$, $\mathfrak{C}^A$, and $\mathfrak{D}^A$ we substitute their respective values into the definition-equation for the deflection w. For the symmetrical moment loading we thus use equation (5) to obtain

$$(19)\quad w^S(x,y) = \sum_m -\frac{M_m b^2}{\varrho_P}\,\Phi^S(y)_m\sin\frac{m\pi x}{l}\,,$$

where

$$(20)\quad \Phi^S(y)_m = \frac{1}{m^2\sigma^2}\,\frac{\mathrm{ch}\,mn'\varphi\cos mt'\varphi\mathfrak{G}_m^S + \mathrm{sh}\,mn'\varphi\sin mt'\varphi\mathfrak{H}_m^S}{\mathfrak{E}_m + \mathfrak{F}_m}\,.$$

Considering next the antisymmetrical case we apply equation (6) and obtain

$$w^A(x, y) = \sum_m - \frac{M_m b^2}{Q_P} \Phi^A(y)_m \sin \frac{m\pi x}{l}, \tag{21}$$

where now

$$\Phi^A(y)_m = \frac{1}{m^2\sigma^2} \frac{\operatorname{sh} mn'\varphi \cos mt'\varphi \mathfrak{G}_m^A + \operatorname{ch} mn'\varphi \sin mt'\varphi \mathfrak{H}_m^A}{\mathfrak{E}_m + \mathfrak{F}_m}. \tag{22}$$

In the latter equations (20) and (22), which define the newly introduced dimensionless coefficients Φ^S and Φ^A, we have used the dimensionless ordinates of location φ.

The factors $\Phi(\vartheta, \alpha, \eta, \varphi)$ are dimensionless; they are depending on the parameter of the lateral stiffness ϑ, on the parameter of torsional stiffness α, on the parameter of contraction ability η, and – naturally – also on the dimensionless parameter

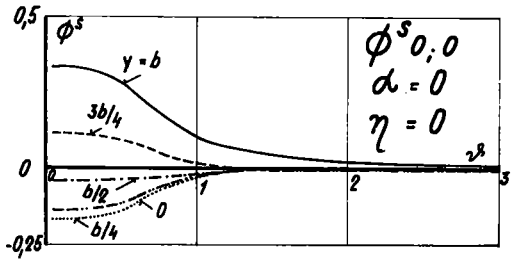

Fig. 2.

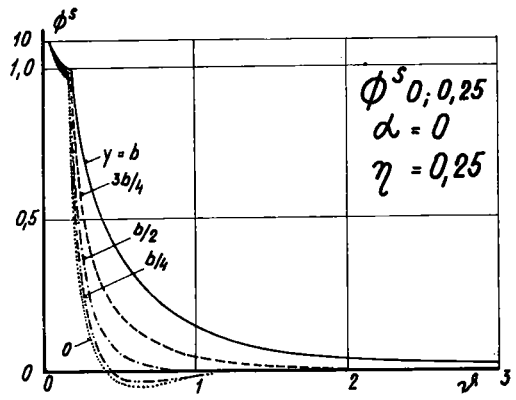

Fig. 3.

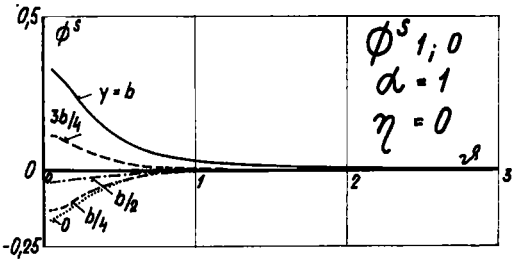

Fig. 4.

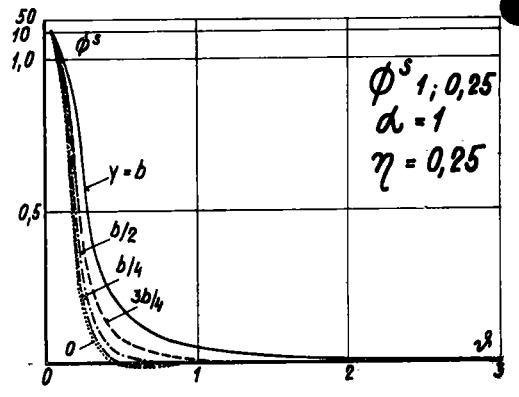

Fig. 5.

of location φ, giving the location of the respective point at which the effect is sought. The values of the dimensionless coefficients $\Phi^S \equiv \Phi^S(y)_1$ and $\Phi^A \equiv \Phi^A(y)_1$ are represented by the graphs in figures 2 and 9. The graphs have been drawn with ϑ as the independent variable for the values $\alpha = 0$, $\alpha = 1$, $\eta = 0$, $\eta = 0{\cdot}25$, and for different point locations φ as given in the figures.

The edge rotations due to the externally applied moments at the edges $y = \pm b$ are given by the first partial derivative of the deflection w with respect to y. Thus for the case of symmetrical edge moments we have

$$\beta^S = \sum_m - \frac{M_m b}{\varrho_P} \Gamma^S(b)_m \sin \frac{m\pi x}{l}, \tag{23}$$

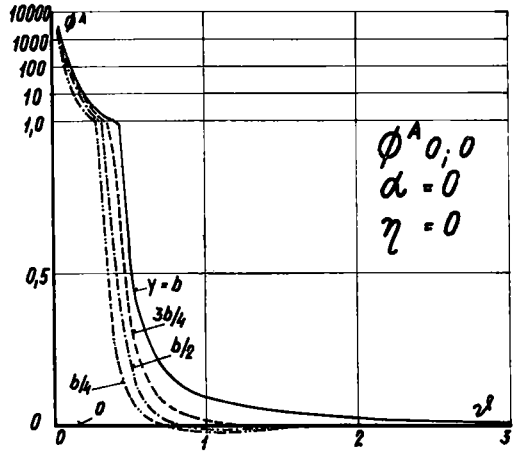

Fig. 6.

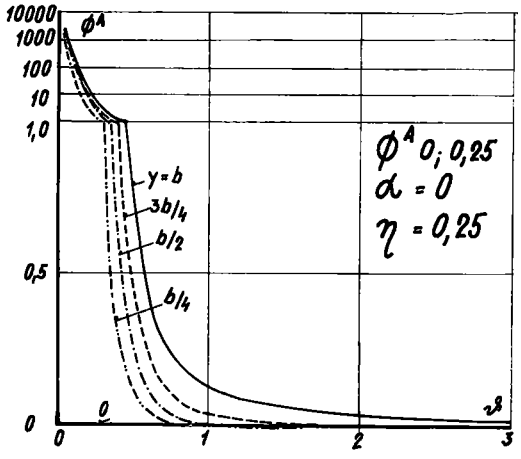

Fig. 7.

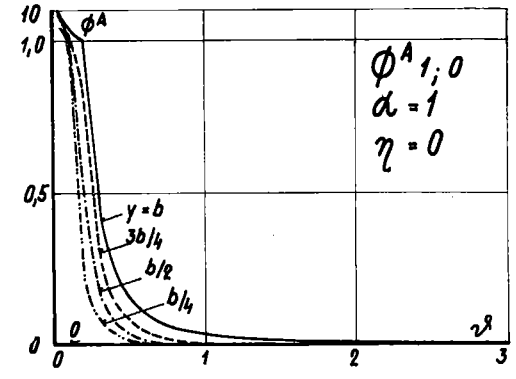

Fig. 8.

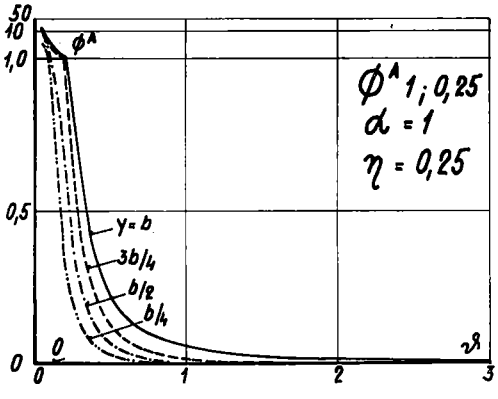

Fig. 9.

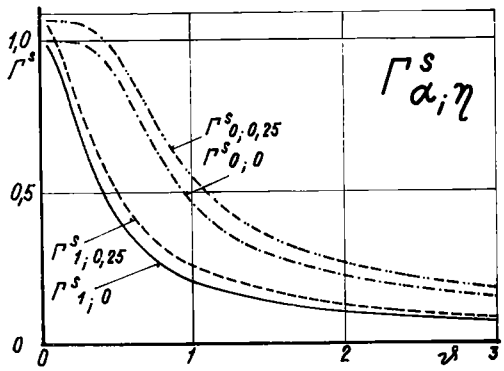

Fig. 10.

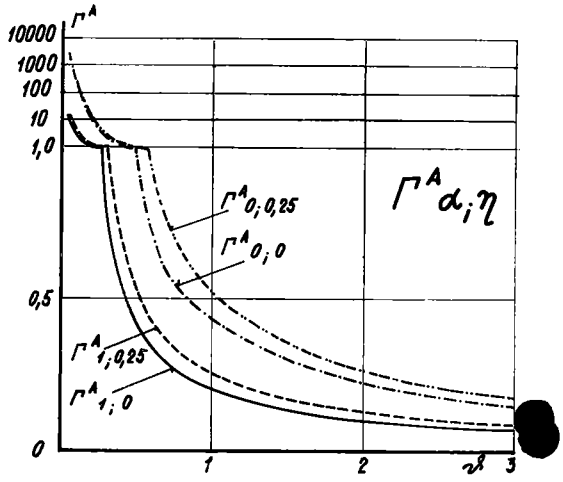

Fig. 11.

where

(24)
$$\Gamma^S(b)_m = \frac{\sqrt{\left(\frac{1-\varepsilon}{2}\right)}}{m\sigma} \frac{\operatorname{sh} mn'\pi \cos mt'\pi(a\mathfrak{G}^S_m + \mathfrak{H}^S_m)}{\mathfrak{E}_m + \mathfrak{F}_m} + \frac{\operatorname{ch} mn'\pi \sin mt'\pi(a\mathfrak{H}^S_m - \mathfrak{G}^S_m)}{\mathfrak{E}_m + \mathfrak{F}_m},$$

while for the case of antisymmetrical edge moments we obtain

(25)
$$\beta^A = \sum_m - \frac{M_m b}{\varrho_P} \Gamma^A(b)_m \sin \frac{m\pi x}{l},$$

where

(26)
$$\Gamma^A(b)_m = \frac{\sqrt{\left(\frac{1-\varepsilon}{2}\right)}}{m\sigma} \frac{\operatorname{ch} mn'\pi \cos mt'\pi(\mathfrak{G}^A_m a + \mathfrak{H}^A_m)}{\mathfrak{E}_m + \mathfrak{F}_m} + \frac{\operatorname{sh} mn'\pi \sin mt'\pi(a\mathfrak{H}^A_m - \mathfrak{G}^A_m)}{\mathfrak{E}_m + \mathfrak{F}_m}.$$

The factors $\Gamma^S(\vartheta, \alpha, \eta)$ and $\Gamma^A(\vartheta, \alpha, \eta)$ as defined by (24) and (25), respectively, are dimensionless, and again they depend on the parameter of lateral stiffness ϑ, on the parameter of torsional stiffness α, and on the parameter of contraction ability η. The numerical values of the dimensionless coefficients $\Gamma^S \equiv \Gamma^S(b)_1$, $\Gamma^A \equiv \Gamma^A(b)_1$, have been computed for $\alpha = 0$, $\alpha = 1$, and for $\eta = 0{\cdot}25$; the results of the computations are represented by the graphs of fig. 10 and 11, the graphs being drawn for the location ordinates.

Finally, the transverse bending moments due to the edges being loaded by symmetrical edge-moments, are obtained as

(27)
$$M^S_P = \sum_m M_m \Psi^S(y)_m \sin \frac{m\pi x}{l}$$

where

$$(28)\qquad \Psi^S(y)_m = \frac{\operatorname{ch} mn'\varphi \cos mt'\varphi[(\varepsilon-\eta)\,\mathfrak{G}_m^S + \sqrt{(1-\varepsilon^2)}\,\mathfrak{H}_m^S]}{\mathfrak{E}_m + \mathfrak{F}_m} +$$

$$+ \frac{\operatorname{sh} mn'\varphi \sin mt'\varphi[(\varepsilon-\eta)\,\mathfrak{H}_m^S - \sqrt{(1-\varepsilon^2)}\,\mathfrak{G}_m^S]}{\mathfrak{E}_m + \mathfrak{F}_m}.$$

Similarly, when the antisymmetrical edge moments are applied, we find for the transverse bending moments the expression

$$(29)\qquad M_P^A = \sum_m M_m \Psi^A(y)_m \sin\frac{m\pi x}{l},$$

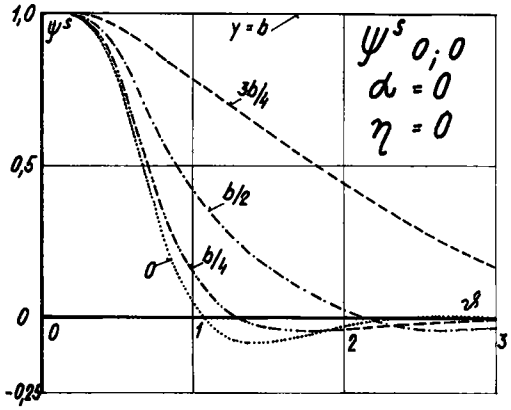

Fig. 12.

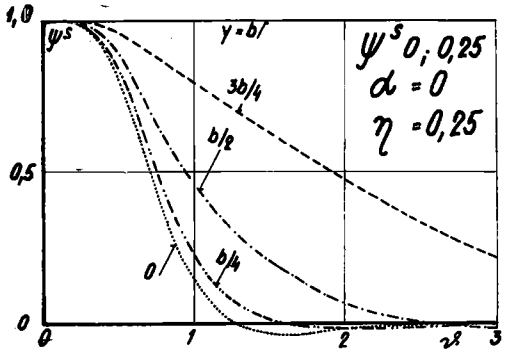

Fig. 13.

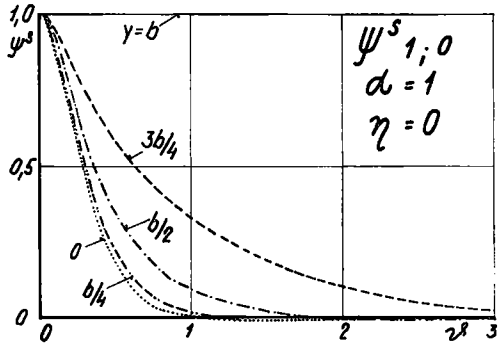

Fig. 14.

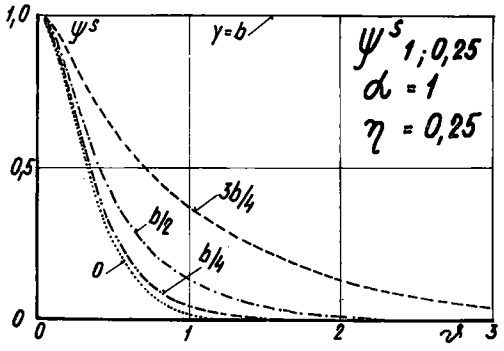

Fig. 15.

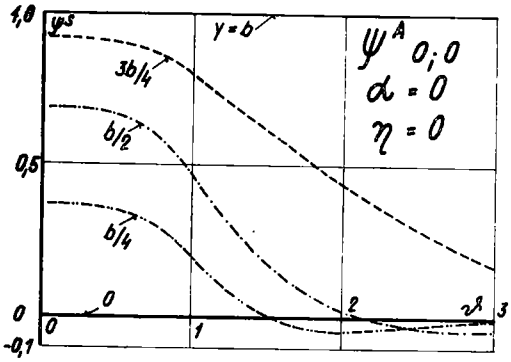

Fig. 16.

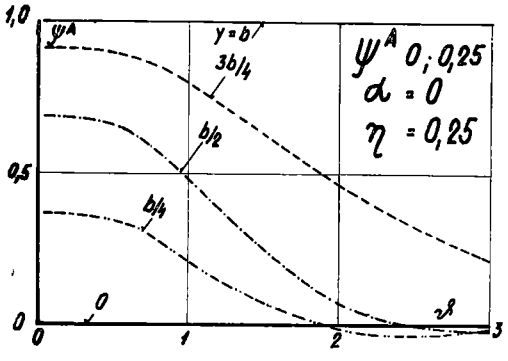

Fig. 17.

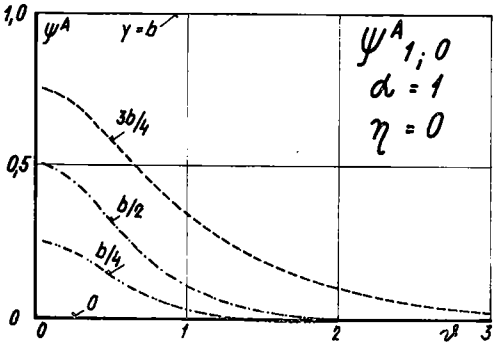

Fig. 18.

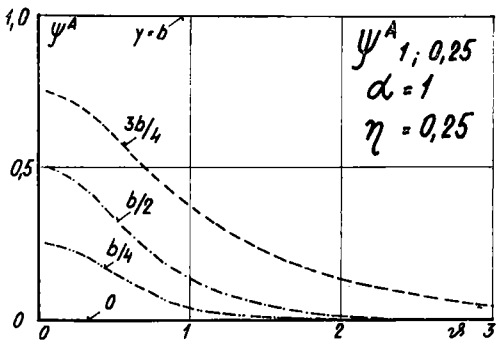

Fig. 19.

where

$$\Psi^A(y)_m = \frac{\operatorname{sh} mn'\varphi \cos mt'\varphi[\mathfrak{G}_m^A(\varepsilon - \eta) + \mathfrak{H}_m^A\sqrt{(1-\varepsilon^2)}]}{\mathfrak{E}_m - \mathfrak{F}_m} + \tag{30}$$

$$+ \frac{\operatorname{ch} mn'\varphi \sin mt'\varphi[\mathfrak{H}_m^A(\varepsilon - \eta) - \mathfrak{G}_m^A\sqrt{(1-\varepsilon^2)}]}{\mathfrak{E}_m - \mathfrak{F}_m}.$$

Equations (28) and (30) define the last two of the factors which are needed in the complete solution to the problem of edge stiffening. The dimensionless factors $\Psi(\vartheta, \alpha, \eta, \varphi)$ depend again on the parameter of lateral stiffness ϑ, on the parameter of torsional stiffness α, on the parameter of contraction ability η, and – of necessity – on the parameter φ which defined the location of the respective point for which the transverse bending moment is required. With ϑ as independent variable the dimensionless factors $\Psi^S \equiv \Psi^S(y)_1$ and $\Psi^A \equiv \Psi^A(y)_1$ are represented by the graphs shown in the figures 12 to 19. The graphs have been constructed for $\alpha = 0$, $\alpha = 1$, $\eta = 0$, and $\eta = 0{\cdot}25$, as well as for different values of φ, as shown directly in the diagrams.

Table 1. Interpolation Function $F(k)$

1-st degree interpolation — precise

Factor	ϑ	Interpolation for η		ϑ	Interpolation for α
		$\alpha = 0$	$\alpha = 1$		
Φ^S	0·05 ↓ 5·0	(4η)	(4η)	0·05	α
				0·10 ↓ 0·55	$\alpha^{1\cdot07-1\cdot18\vartheta}$
				0·60 ↓ 5·0	$\alpha^{1\cdot14}\cdot e^{(1-\alpha)}$
Φ^A	0·05	$(4\eta)^2$	(4η)	0·05 ↓ 0·65	$\alpha^{(0\cdot73\vartheta+0\cdot68)}\cdot e^{(1-\alpha)}$
	0·10 ↓ 0·30	$(4\eta)^{2\cdot15-2\cdot51\vartheta}$			
	0·35 ↓ 5·0	(4η)		0·70 ↓ 5·0	$\alpha^{1\cdot14}\cdot e^{(1-\alpha)}$
Γ^S	0·05 ↓ 0·45	$(4\eta)^2$	$(4\eta)^{1\cdot072\vartheta-0\cdot23}$	0·05	α
				0·10 ↓ 0·40	$\alpha^{(1\cdot07-1\cdot18\vartheta)}$
	0.50 ↓ 0·95	$(4\eta)^{1\cdot26\vartheta-0\cdot55}$	(4η)	0·45 ↓ 0·60	$\alpha^{(0\cdot79-0\cdot53\vartheta)}$
	1·50 ↓ 5·0	$(4\eta)^{1\cdot32}$		0·65 ↓ 5·0	$\sqrt{\alpha}$
Γ^A	0·05	$(4\eta)^2$	(4η)	0·05	$\alpha^{0\cdot0073}$
	0·10 ↓ 5·0	(4η)		0·10 ↓ 0·55	$\alpha^{(0\cdot94\vartheta-0\cdot066)}$
				0·60 ↓ 5·0	$\sqrt{\alpha}$

Table 1. (cont.)

Factor	ϑ	Interpolation for η		ϑ	Interpolation for α
		$\alpha = 0$	$\alpha = 1$		
Ψ^S	0·05 ↓ 0·20	(4η)	$(4\eta)^{0\cdot86}$	0·05	α
	0·25 ↓ 0·60		$(4\eta)^{0\cdot91}$	0·10 ↓ 0·55	$\alpha e^{(0\cdot12-1\cdot55\vartheta)}$
	0·65 ↓ 5·0		$(4\eta)^{0\cdot94}$	0·60 ↓ 5·0	$\alpha^{1\cdot11} \cdot e^{(1-\alpha)}$
Ψ^A	0·05 ↓ 5.0	(4η)	(4η)	0·05 ↓ 0·40	$\alpha^{(1\cdot33\vartheta-0\cdot049)}$
				0·45 ↓ 0·95	$\sqrt{\alpha}$
				1·00 ↓ 5·0	$\alpha^{1\cdot11} \cdot e^{(1-\alpha)}$

As has been elsewhere derived, for anyone of the factors Φ, Γ, or Ψ, their respective values $\Phi(y)_m$, $\Gamma(y)_m$, $\Psi(y)_m$, which correspond to the m-th term of the pertaining Fourier series are identical to the values $\Phi(y)_1$, $\Gamma(y)_1$, $\Psi(y)_1$, pertaining to the first term of the respective series, but developped with the use of the reduced magnitude $m\vartheta$ of the parameter of lateral stiffness. For practical design purposes the effects due to the outer beams having different stiffness (as compared with the intermediate beams) are – in practically all cases of interest – with sufficient accuracy obtained with only the first term of the respective Fourier series.

To evaluate the dimensionless factors for intermediate values of α and η, we can either employ the computation by means of the above given theoretical formulae, but – since such a procedure would be rather tedious, we find the respective values by means of the interpolation formula

$$\mathfrak{X}_k = \mathfrak{X}_{\min} + (\mathfrak{X}_{\max} - \mathfrak{X}_{\min})\, F(k)\,. \tag{31}$$

Here, the symbol $F(k)$ denotes the respective functions of interpolation, tabulated in the two tables below. The numerical coefficients in the functions $F(k)$ have been

Table 2. Interpolation Function

2-nd degree interpolation — simplified

Factor	ϑ	Interpolation for η		ϑ	Interpolation for α
		$\alpha = 0$	$\alpha = 1$		
Φ^S	0·05 ↓ 5·0	(4η)	(4η)	0·05 0·35	$\alpha^{(1\cdot07-1\cdot18\vartheta)}$
				0·40 5·0	$\sqrt{\alpha}$
Φ^A	0·05 ↓ 5.0	(4η)	(4η)	0·05 0·35	$\alpha^{(0\cdot73\vartheta+0\cdot68)} \cdot e^{(1-\alpha)}$
				0·40 5·0	$\alpha^{1\cdot14} \cdot e^{(1-\alpha)}$
Γ^S	0·05 ↓ 5·0	(4η)	(4η)	0·05 0·35	$\alpha^{(1\cdot07-1\cdot18\vartheta)}$
				0·40 5.0	$\sqrt{\alpha}$
Γ^A	0·05 ↓ 5.0	(4η)	(4η)	0·05	$\alpha^{0\cdot0073}$
				0.10 0·35	$\alpha^{(0\cdot94\vartheta-0\cdot07)}$
				0·40 5·0	$\sqrt{\alpha}$
Ψ^S	0·05 ↓ 5·0	(4η)	(4η)	0·05 5·0	$\sqrt{\alpha}$
Ψ^A	0·05 ↓ 5·0	(4η)	(4η)	0·05 0·35	$\alpha^{(1\cdot33\vartheta-0\cdot05}$
				0·40 5·0	$\sqrt{\alpha}$

computed (on the basis of a considerable number of analysed cases) so as to give an error of less than 2·5% for anyone of the dimensionless factors (1-st degree interpolation), or to give an error of less than 2·5% in all the governing (i.e. maximum) values in all the dimensionless factors for any arbitrary combination of ϑ, α and η (2-nd degree interpolation — see [2]). The respective formulae defining the functions of interpolation are given in Tables 1 and 2 below.

4. COMPLETE SOLUTION FOR SYSTEMS WITH EDGE BEAMS

We consider the system shown in Fig. 20: the length of span is l, the width of the structure is $2b$, and at both the ends of the span we assume the longitudinal beams to be interconnected by means of supporting cross beams, stiff enough to prevent any transverse rotation over the cross-section of the bridge deck. The rigidity factors per unit of distance are ϱ_T, γ_T and ϱ_P, γ_P for the longitudinal and the lateral directions, respectively. Finally, we assume that the two edge beams (Fig. 20) are markedly stiffer than the interior beams, the rigidity factors of anyone of the two edge beams being $\bar{\varrho}_T$ (flexure) and $\bar{\gamma}_T$ (torsion).

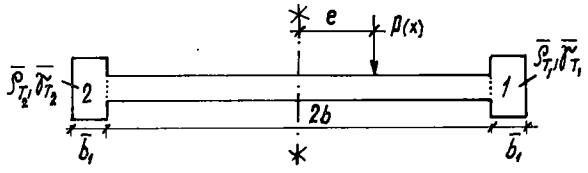

Fig. 20.

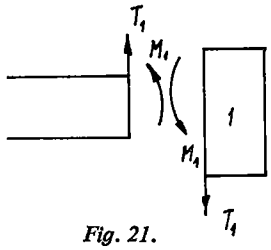

Fig. 21.

The analysis of the just described structurally orthotropical system will be performed by the method as indicated in [3]. First we assume that the edge beams are separated (by longitudinal gaps) from the middle part of the bridge deck. The mutual interaction of the parts is represented by the internal components T and M (see Fig. 21). For any case of external load varying harmonically along X, also the internal forces as produced by such a load will be in the X-direction harmonic.

Next we perform partial analysis for the interior part of the separately taken bridge deck, idealizing this structural part by an equivalent orthotropic plate. The edge loads due to the components T and M are assumed as additional external loads, and they are thus considered as to act simultaneously with the true external load p. For the total external load (i.e. the true load p and the assumed additional load due to T and M) we have to compute the deflections w as well as the transverse rotations β which such total load induces at the two edges $y = \pm b$. Using only the first terms of the respective Fourier expansions, we apply the dimensionless parameters K (see [1]) and Φ (defined in the preceding chapter) to find the vertical deflection w at the edges $y = \pm b$ to be given as follows

$$(32)\quad w(x, y = b) = \frac{l^4}{\pi^3 \varrho_T} \sin\frac{\pi x}{l}\left[\frac{p_1}{2b} K(e, b) - \frac{T_1}{2b} K(b, b) - \frac{T_2}{2b} K(b, b)\right] -$$

$$- \frac{b^2}{2\varrho_P} \sin\frac{\pi x}{\varrho}\left[(M_1 + M_2)\, \Phi^S(b) + (M_1 - M_2)\, \Phi^A(b)\right],$$

$$w(x, y = -b) = \frac{l^4}{\pi^3 \varrho_T} \sin\frac{\pi x}{l}\left[\frac{p_1}{2b} K(e, -b) - \frac{T_1}{2b} K(-b, b) - \frac{T_2}{2b} K(-b, -b)\right] -$$

$$- \frac{b^2}{2\varrho_P} \sin\frac{\pi x}{l}\left[(M_1 + M_2)\, \Phi^S(b) - (M_1 - M_2)\, \Phi^A(b)\right].$$

In equation (32), instead of the edge moments M_1 and M_2 (applied at the edges $y = \pm b$ respectively) their symmetrical equivalent $(M_1 + M_2)/2$ and their anti-symmetrical equivalents $(M_1 - M_2)/2$ have been used. The end rotations at the edges of the equivalent orthotropic plate are, for the same total external load as in the foregoing case, defined by the two equations

$$(33)\quad \beta(x, y = b) = \frac{l^4}{4\sqrt{(\varrho_T \varrho_P)}\, \pi^2} \sin\frac{\pi x}{l}\left[p\, \tau(e, b) - T_1\, \tau(b, b) - T_2\, \tau(-b, b)\right] -$$

$$- \frac{b}{2\varrho_P} \sin\frac{\pi x}{l}\left[(M_1 + M_2)\, \Gamma^S_{(b)} + (M_1 - M_2)\, \Gamma^A_{(b)}\right]$$

and

$$\beta(x, y = -b) = \frac{l^4}{4\sqrt{(\varrho_T \varrho_P)}\, \pi^2} \sin\frac{\pi x}{l}\left[p\, \tau(e, -b) - T_1\, \tau(b, -b) - T_2\, \tau(-b, -b)\right] -$$

$$- \frac{b}{2\varrho_P} \sin\frac{\pi x}{l}\left[(M_1 + M_2)\, \Gamma^S_{(b)} - (M_1 - M_2)\, \Gamma^A_{(b)}\right].$$

Now we have to compute the vertical deflection for the edge beams assumed to be separated from the middle part of the bridge deck. Using again the Fourier series and considering only the first term of the series we find, that in case of an externaly applied harmonic load T, the corresponding deflections of edge beams "1" and "2" (Fig. 20, 21) are

$$(34)\qquad w(x)_1 = \frac{l^4}{\pi^4 \bar{\varrho}_{T_1}} T_1 \sin\frac{\pi x}{l},$$

$$w(x)_2 = \frac{l^4}{\pi^4 \bar{\varrho}_{T_2}} T_2 \sin\frac{\pi x}{l}.$$

An externally applied torque $[M_1 - T_1(\bar{b}_1/2)] \sin \pi x/l$ induces transverse rotation of the edge beam section equal to the angle of twist produced by the same torque. At any ordinate X the transverse rotation of edge beam "1" is thus represented

by the equation

$$(35a) \qquad \varphi(x)_1 = \frac{\left(M_1 - T_1 \frac{\bar{b}_1}{2}\right) \frac{l}{\pi} \int_0^x \cos \frac{\pi x}{l} \, dx}{\bar{\gamma}_{T_1}} = \frac{\left(M_1 - T_1 \frac{\bar{b}_1}{2}\right) \frac{l^2}{\pi^2}}{\bar{\gamma}_{T_1}} \sin \frac{\pi x}{l} \; ^1).$$

For the transverse rotation of edge beam "2" (see Fig. 20, 21) we obtain, similarly, the equation

$$(35b) \qquad \varphi(x)_2 = \frac{\left(M_2 - T_2 \frac{\bar{b}_1}{2}\right) \frac{l^2}{\pi^2}}{\bar{\gamma}_{T_2}} \sin \frac{\pi x}{l} .$$

Finally, we have to take into account the conditions of continuity at the two edges $y = \pm b$; briefly stated these conditions require that the deformations at the outer two edges of the middle – equivalent – bridge deck be compatible with the deformations at the adjacent surfaces of the two edge beams. The interior part as represented by the equivalent orthotropic plate is, according to the above discussion, subjected to the "total" external load (true load p and assumed additional load due to the components T and M). This total load induces at the outer edges $y = \pm b$ of the equivalent plate vertical deflections w as well as transverse rotations β. Similarly, the vertical deflections and the transverse rotations for each of the two edge beams "1", "2", due now to the action of only the assumed external load by the components T and M, have to be computed, considering either of the edge beams to act separately. The pertaining values of the deflections and of the rotations must be of equal magnitude for the adjacent surfaces of the separately considered elements.

The mathematical representation of the continuity conditions to be met at the two boundaries $y = \pm b$, is as follows

$$(36) \qquad \begin{aligned} w(x, y = b) &= w(x)_1 , \quad \beta(y = b) = \varphi(x)_1 , \\ w(x, y = -b) &= w(x)_2 , \quad \beta(y = -b) = \varphi(x)_2 . \end{aligned}$$

---

[1]) The same expression is obtained for the case of a cantilever beam of length $l/2$, clamped into the rigid cross beam at the support; when the same external torque as in (35a) is applied the angle of twist at any ordinate X is

$$\varphi_{(x)} = \frac{1}{\bar{\gamma}_T} \left[\int_0^x x \left(M - T \frac{\bar{b}_1}{2}\right) \sin \frac{\pi x}{l} dx + x \int_x^{l/2} \left(M - T \frac{\bar{b}_1}{2}\right) \sin \frac{\pi x}{l} dx \right] = \frac{\left(M - T \frac{\bar{b}_1}{2}\right) l^2}{\pi^2 \bar{\gamma}_T} \sin \frac{\pi x}{l}$$

and for $x = l/2$ (midspan) this formula reduces to the simple expression

$$\varphi_{(x)} = \frac{1}{\bar{\gamma}_T} \int_0^{l/2} x \left(M - T \frac{\bar{b}_1}{2}\right) \sin \frac{\pi x}{l} dx = \frac{\left(M - T \frac{\bar{b}_1}{2}\right)}{\pi^2 \bar{\gamma}_T} l^2 .$$

Employing now the boundary conditions (36) together with the set of equations (32), ... to (35) we can compute all the four redundant components T_1, T_2, M_1, and M_2. The computation is especially facilitated if the iterative procedure indicated in [3] is applied. Once the components T and M are known, the further calculation can follow similar pattern as in the method of dimensionless parameters [1]. Since all the stress and deformation components have the same harmonic variation alon X, the solution is with respect to x entirely independent; this may be utilised in such a manner that — for any value of m — the solution at only one ordinate x, say at $x = l/2$ is established, which evidently simplifies all the computation.

A similar procedure can be employed when — in the absence of edge beams at $y = \pm b$ — the section for the two exterior beams is markedly different as compared with the remaining interior beams (see [3]). In [3] also the application of the method of dimensionless parameters is shown for the case of prestressed bridge systems.

References

[1] Bareš, R.: Method of Dimensionless Coefficients for Analysis of Structurally Orthotropic Plane Structures, Acta Technica ČSAV, No. 5, 6, 1973.

[2] Bareš, R.: Interpolationenfunktionen bei der Analyse formorthotroper Flächentragwerke nach der Methode der dimensionslosen Beiwerte, Bericht ÚTAM — ČSAV, 1973.

[3] Bareš, R., Massonnet, Ch.: Le calcul des grillages de poutres et dalles orthotropes selon le méthode Guyon - Massonnet - Bareš, DUNOD, Paris, 1966.

ANALYSIS OF STRUCTUALLY ORTHOTROPIC BRIDGE DECK SYSTEMS WITH STIFFENED OUTER EDGES

The concept of substituting — in the analysis — an equivalent orthotropic plate (with continuously distributed rigidities) for the true, structurally orthotropic plane structure is shown to be of utility also in the analysis of such bridge deck plate-beam grillages, where the outer edge beams are much stiffer in flexure and torsion than the remaining (intermediate) main beams. In bridge construction, such systems are quite frequent since often the edges are stiffened by especial edge beams or the section of the exterior main beams is stiffer than for the intermediate beams, etc. The method of dimensionless parameters [1] is used in the analysis, and it is shown that this approach is considerably expeditious. Theoretical formulae are given for representation of the effects due to transverse edge-moment loads, and some useful dimensionless coefficients are newly introduced and represented by diagrams showing their respective curves of variation for a wide range of the independent parameters; the diagrams have been constructed on the base of numerous computations and the will be found to be of use in practical design calculations.

[Received April 10, 1973]

Ing. Richard Bareš, CSc., Institute of Theoretical and Applied Mechanics, Czechoslovak Academy of Science, Vyšehradská 49, 120 00 Praha 2 - Nové Město.